NJC

PAPER

View Article Online
View Journal | View Issue

Cite this: *New J. Chem.*, 2019, 43, 18559

DBU-functionalized MCM-41-coated nanosized hematite (DBU-F-MCM-41-CNSH): a new magnetically separable basic nanocatalyst for the diastereoselective one-pot four-component synthesis of 2-(*N*-carbamoylacetamide)-substituted 2,3-dihydrothiophenes†

Reza Kordnezhadian, Mohsen Shekouhy * and Ali Khalafi-Nezhad*

Received 14th September 2019,
Accepted 28th October 2019

DOI: 10.1039/c9nj04714j

rsc.li/njc

DBU-functionalized MCM-41-coated nanosized hematite (DBU-F-MCM-41-CNSH) was prepared as a new magnetically separable mesoporous nanomaterial and was characterized by various techniques such as FT-IR, XRD, HR-TEM, FESEM, BET, VSM and elemental analyses (CHN and ICP). The synthesized magnetic mesoporous nanomaterial was applied successfully as a basic nanocatalyst for the diastereoselective synthesis of 2-(*N*-carbamoylacetamide)-substituted 2,3-dihydrothiophenes through a one-pot four-component reaction of aryl aldehydes, primary and secondary amines, 1,3-thiazolidinedione and malononiterile in a 1 : 2 v/v mixture of EtOH/H_2O at 60 °C. Using this method, all desired products were obtained in good to excellent yields (83–94%) after short times (25–45 min). The chemical and physical stability of the catalyst was proved by studying its chemical structure using the same analyses after the 8th reuse.

Introduction

Nowadays, acquisition of a more innovative green strategy for more effective synthesis of industrial and pharmaceutical compounds is a challenging area of research. One of the methods that has recently been prioritized is that of multi-component reactions (MCRs), which produce the desired product in only one step.[1,2] As a result, this method is practically straightforward, maximizes the yield, minimizes the required cost and energy and reduces waste and the reaction time period. Moreover, various products can be achieved only by changing the starting materials, whereby the generality of the synthesis is enhanced and the products can be greatly diversified. Furthermore, the starting materials for MCRs are almost all easily accessible. In addition, MCRs have shown their magnificent capability of accomplishing the synthesis of highly complex natural products as well as large-scale production of drug candidates far more easily than the traditional stepwise methods. This provides medicinal chemists with a powerful tool to connect the space of biological targets with the relevant chemistry.[3,4]

The ongoing discovery of novel MCRs is a promising area of research, yielding novel chemical scaffolds for drug discovery efforts. MCRs have been successfully applied for the synthesis of several classes of heterocyclic compounds.[5] One important group of these heterocyclic compounds is dihydrothiophenes. Dihydrothiophenes have turned into the main pharmacophores in lots of considerably biologically active compounds and pharmaceutical agents.[6–8] They are also used as a versatile class of synthetic intermediates.[8–10] There are just a few reported multi-component methods for the synthesis of dihydrothiphenes.[8,11,12] However, these routes also possess some striking weaknesses and limitations including low diversity of available starting materials,[11–14] very long reaction times,[11,13–17] very low yields of products,[11–17] restrictions to special instruments,[12] and no reusability of the applied catalysts.[15–17] Therefore, exploring a more efficient and environmentally benign procedure is still in demand. It is not a false claim to say that the use of the catalytic methodologies applied in MCRs has led to easier and straightforward access to new heterocyclic libraries of small molecules[18] with huge potential for biological applications.[19] So, the design and preparation of more efficient catalytic systems for MCRs can be effective in the process of developing MCRs for the synthesis of potentially biologically active compounds.

1,8-Diazabicyclo[5.4.0]undec-7-ene (DBU) is an amidine compound which has achieved great fame because of its unique

Department of Chemistry, College of Sciences, Shiraz University, Shiraz 71454, Iran. E-mail: m.shekouhy@shirazu.ac.ir, Khalafi@shirazu.ac.ir

† Electronic supplementary information (ESI) available. See DOI: 10.1039/c9nj04714j

features and has been used as a base catalyst for many important chemical transformations so far.[20–25] Nonetheless, DBU possesses some drawbacks which are far from the concepts of green chemistry such as high toxicity (DBU LD_{50} = 189 mg kg^{-1}, oral rat) in combination with non-recoverability. In other words, the non-recoverability feature of DBU in conjunction with its toxicity turns it into disastrous harmful waste.[26] Therefore, there is urgent demand to fix these weaknesses.

Recently, nanocatalysts have been the center of attention of many active research groups as they contribute numerous merits over homogeneous and traditional heterogeneous catalytic systems.

Nanocatalysts have high accessible surface area-to-volume ratios, which in turn enhance the reactivity of these catalysts and make it possible to use smaller amounts of them for chemical transformations.[27] Moreover, the use of smaller amounts of these catalysts makes them comparatively more cost-effective and also prevents the disposal of more hazardous waste into the environment.[27] Furthermore, the features of nanocatalysts such as size, shape, composition and morphology could be manipulated if required.[27] Accordingly, some new catalytic systems with DBU immobilized on the surface of nano compounds have been reported so far, misleadingly considered to be remarkable progress.[28–31] As the separation and recovery steps for nanocatalysts require ultrafiltration and high speed centrifugation methods and these highly expensive tedious methods are not completely efficient, the recoverability of the nanocatalysts is still an unresolved issue. In order to overcome the above-mentioned issues, implementation of magnetic nanoparticles (MNPs) could be a key solution since they can be readily and efficiently separated from the reaction mixtures by a simple external magnetic field.[32]

Considering these facts, as the sequel of our recent studies on the design, preparation and application of more benign, efficient and reusable catalysts for the synthesis of organic compounds,[33] and as the sequel of our recent efforts to convert DBU as a liquid non-reusable base catalyst to a more benign solid reusable catalytic system,[34] we herein intend to introduce DBU-functionalized MCM-41-coated nanosized hematite (DBU-F-MCM-41-CNSH) as a new highly efficient, magnetically separable and reusable mesoporous nanocatalyst for one-pot four-component synthesis of 2-(*N*-carbamoylacetamide)-substituted 2,3-dihydrothiophenes (**5aa–5bj**) (Scheme 1).

Experimental

General information

All chemicals were purchased from Fluka, Merck and Aldrich chemical companies. The reaction monitoring was accomplished by TLC on silica gel PolyGram SILG/UV254 plates. The eluent solvents were petroleum ether, ethyl acetate or a mixture of them. All yields refer to isolated products after the indicated purification methods. The products were characterized through their spectral data analysis. Melting points were determined in open capillary tubes with a Büchi B-545 melting point apparatus. ^{1}H NMR (250 MHz) and ^{13}C NMR (100 MHz) spectra were run on a Bruker Avance DRX-250 and Bruker Avance DRX-400 respectively in pure $CDCl_3$ or DMSO-d_6 solvents. All chemical shifts are given on the δ scale in parts per million (ppm) and J in Hz. IR spectroscopy (Shimadzu FT-IR 8300 and Perkin Elemer FT-IR RX 1 spectrophotometers), in cm^{-1}, was employed for characterization of the compounds. Microanalysis was performed on a PerkinElmer 240-B microanalyzer. Inductively coupled plasma (ICP) analysis was performed using an ICP analyzer (Varian, Vista-Pro). XRD patterns were recorded on a Bruker D8 ADVANCE X-ray diffractometer using nickel filtered Cu K_α radiation (λ = 1.5406 Å). Scanning electron microscopy (SEM) was performed using a KYKY-EM3200 instrument. High resolution transmission electron microscopy (HR-TEM) was performed with a JEOL, JEM-2100F, 200 kV TEM. VSM curves were recorded

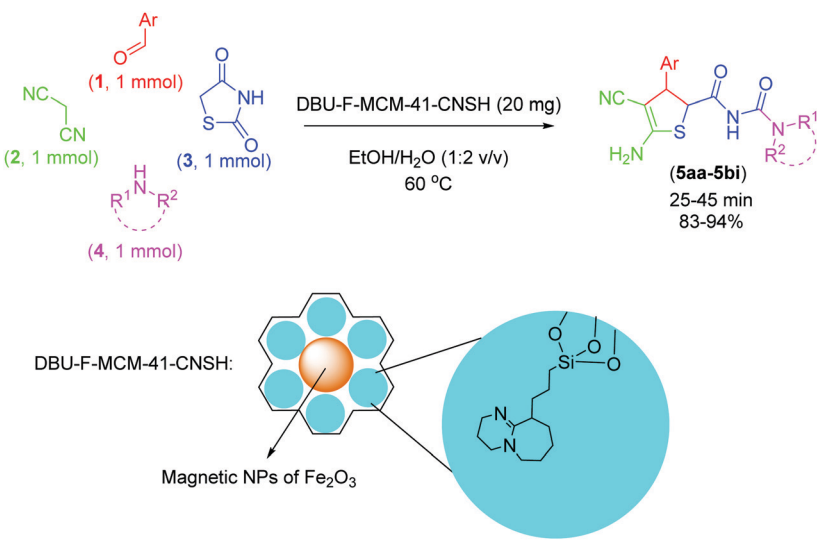

Scheme 1 The one-pot four-component synthesis of 2-(*N*-carbamoylacetamide)-substituted 2,3-dihydrothiophenes (**5aa–5bj**) in the presence of DBU-F-MCM-41-CNSH as a new magnetically separable mesoporous basic nanocatalyst.

using a vibrating sample magnetometer model VSM 4 Daghigh Meghnatis Kashan Co. N_2 adsorption–desorption isotherms were obtained at 77 K using a micrometritics instrument model Asap2020.

The synthesis of 10-(3-(trimethoxysilyl)propyl)-2,3,4,6,7,8,9,10-octahydropyrimido[1,2-*a*]azepine (9)

Anhydrous DBU (10 mmol, 1.52 g) was added to dry tetrahydrofuran (50 mL) under a nitrogen atmosphere in a 250 mL three neck round-bottom flask equipped with a dropping funnel. *n*-Butyllithium in *n*-hexane (15 mmol, 2.66 M) was slowly added from the dropping funnel (10 min) at 0 °C, and the mixture was magnetically stirred for 1 h. Then (3-chloropropyl)-trimethoxysilane (10 mmol, 1.98 g) in tetrahydrofuran (25 mL) was slowly added from the dropping funnel (10 min) and the mixture was stirred for 12 h at room temperature. After this time, in order to quench the mixture, methanol (*ca.* 20 mL) was added, the solvent was evaporated under reduced pressure and the resulting viscous oil (pale yellow) was washed with diethyl ether (25 mL, 2 times) and dried under reduced pressure for 24 h and the desired product was obtained as a yellow viscous oil (98%, 3.08 g). ^{1}H NMR (250 MHz, $CDCl_3$): δ (ppm) 0.59 (t, J = 5.5 Hz, 2H), 0.87–1.03 (m, 4H), 1.57–1.83 (m, 8H), 2.33–2.41 (m, 1H), 3.17–3.27 (m, 6H), 3.50 (s, 9H).

The synthesis of Fe_3O_4 magnetic nanoparticles

$FeCl_3{\cdot}6H_2O$ (20 mmol, 5.40 g) and $FeCl_2{\cdot}4H_2O$ (10 mmol, 1.98 g) were dissolved in deionized water (30 mL). The solution was heated to 60 °C under nitrogen gas and vigorous mechanical stirring with a glassware stirrer for 30 min, followed by the slow addition of a NaOH solution (1.5 M, 250 mL). During the whole process, the solution temperature was maintained at 60 °C and the pH was kept above 10.0. Then, the obtained precipitate was separated from the reaction medium by an external magnet and washed with deionized water (100 mL, 4 times). The obtained solid was dried under reduced pressure for 24 h and Fe_3O_4 magnetic nanoparticles were obtained as a dark brown solid (2.29 g).

The synthesis of MCM-41-coated α-Fe_2O_3 nanoparticles (11)

The synthesis of MCM-41-coated α-Fe_2O_3 nanoparticles was carried out using tetraethyl orthosilicate (TEOS) as the Si source, cetyltrimethylammonium bromide (CTAB) as the surfactant template, Fe_3O_4 nanoparticles as the magnetic core and ammonia as the pH control agent with a gel composition of $Si : Fe : CTAB : NH_4OH : H_2O$ = 1.00 : 0.075 : 0.127 : 0.623 : 508. In a typical synthesis procedure, Fe_3O_4 magnetic nanoparticles (0.13 g) were dispersed in deionized water (200 mL) under sonication for 15 min and then CTAB (1.04 g) was dissolved in this solution under stirring using a mechanical mixer. The mixture temperature was increased up to 60 °C and kept at this temperature for 15 min. TEOS (22.5 mmol, ≈4.66 g) was added dropwise to the obtained mixture and the pH was adjusted to 10.5 by adding 25 wt% ammonia solution and the obtained mixture was stirred mechanically using a glassware stirrer for 12 h at room temperature. The gel was separated using an external magnet and washed with ethanol (5 mL, three times) and deionized water (10 mL, three times). The solid was dried at 120 °C for 2 h and calcinated in air at 550 °C for 4 h to give MCM-41-coated α-Fe_2O_3 nanoparticles as an orange brown powder (1.40 g).

The synthesis of DBU-F-MCM-41-CNSH (12)

To a double neck round-bottom flask equipped with a mechanical stirrer and a condenser, anhydrous toluene (25 mL) and dehydrated purely MCM-41-coated α-Fe_2O_3 nanoparticles (1.00 g) were added and the insoluble particles were truly dispersed by sonication for 20 min. After this time, 10-(3-(trimethoxysilyl)propyl)-2,3,4,6,7,8,9,10-octahydropyrimido[1,2-*a*]azepine (2 mmol, 0.62 g) and pyridine (0.5 mmol, ≈0.04 g) were added and the resulting mixture was vigorously stirred using a glassware mechanical stirrer at reflux temperature for 6 h. After this time, the reaction mixture was cooled to room temperature and the powder was separated using an external magnet, washed with ethanol (20 mL, three times) and water (20 mL, three times) and dried at 120 °C for 4 h. DBU-F-MCM-41-CNSH was obtained as an orange brown powder (1.28 g).

The general procedure for the one-pot four-component synthesis of 2-(*N*-carbamoylacetamide)-substituted 2,3-dihydrothiophenes (5aa–5bi) in the presence of DBU-F-MCM-41-CNSH

Aryl aldehyde (1.0 mmol) and malononitrile (1.0 mmol, 0.06 g) were added to a 25 mL round-bottom flask containing a suspension of DBU-F-MCM-41-CNSH (0.020 g) in EtOH/H_2O 1 : 2 (10 mL) and the resulting mixture was stirred at 60 °C for 2 min. Then, 1,3-thiazolidinedione (1.0 mmol, 0.11 g) and the amine (1.0 mmol) were added and the reaction mixture was stirred at the same temperature and the progress of the reaction was followed by TLC. After completion of the reaction, as indicated by TLC, the reaction mixture was cooled to room temperature and filtered. The separated solids were dissolved in hot ethanol (20 mL) and the remaining insoluble catalyst was separated using an external magnet. Small amounts of catalyst that passed the filter were also separated using an external magnet and added to the separated catalyst from the hot ethanol, washed well with hot ethanol (5 mL, 2 times), dried at 120 °C and kept for another use (0.0197 g of the catalyst was recovered successfully). The hot solution of crude products in ethanol was left to stand at room temperature overnight and during this time the pure products were precipitated slowly.

Results and discussion

At the beginning, 10-(3-(trimethoxysilyl)propyl)-2,3,4,6,7,8,9,10-octahydropyrimido[1,2-*a*]azepine (**8**) was synthesized by the reaction of *in situ* formed 7-lithium-1,8-diazabicyclo[5.4.0]-undec-7-ene (**6**) and (3-chloropropyl)trimethoxysilane (**7**) in dry THF (Scheme 2). The structure of the synthesized 10-(3-(trimethoxysilyl)propyl)-2,3,4,6,7,8,9,10-octahydropyrimido[1,2-*a*]azepine (**8**) was demonstrated by ^{1}H-NMR spectroscopy (ESI,† Fig. S1).

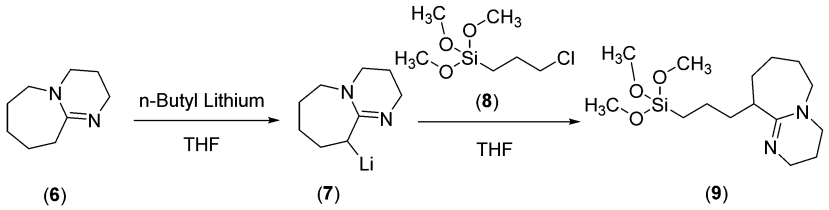

Scheme 2 The synthesis of (3-(trimethoxysilyl)propyl)-2,3,4,6,7,8,9,10-octahydropyrimido[1,2-*a*]azepine (**8**).

In the ^{1}H-NMR spectrum of (3-(trimethoxysilyl)propyl)-2,3,4,6,7,8,9,10-octahydropyrimido[1,2-*a*]azepine (**8**), hydrogen nuclei α to silicon appeared as a triplet at 0.59 ppm. Hydrogen nuclei β and γ to silicon appeared as multiplets between 0.87 and 1.03 ppm. Hydrogen nuclei connected to carbons no. 3, 4, 5 and 10 in the DBU moiety appeared as a multiplet between 1.57 and 1.83 ppm. The hydrogen nucleus connected to carbon no. 6 in the DBU moiety appeared as a multiplet between 2.33 and 2.41 ppm. Hydrogen nuclei connected to carbons no. 9 and 11 in the DBU moiety appeared as a multiplet between 3.17 and 3.27 ppm and hydrogen nuclei of the three methoxy groups appeared as a singlet at 3.50 ppm.

In the next step, the magnetically separable mesoporous support (MCM-41-coated nanosized hematite) was prepared with the formation of MCM-41 around the γ-Fe_3O_4 magnetic nanoparticles (**9**) and calcination at 550 °C under an air atmosphere. For this, MCM-41-coated γ-Fe_3O_4 nanoparticles were synthesized at room temperature with the use of tetraethyl orthosilicate (TEOS) (**10**) as the Si source, cetyltrimethylammonium bromide (CTAB) as the surfactant template, γ-Fe_3O_4 nanoparticles (**9**) as the magnetic core and ammonia as the pH control agent with a gel composition of Si : Fe : CTAB : NH_4OH : H_2O = 1.00 : 0.075 : 0.127 : 0.623 : 508 followed by calcination at 550 °C under an air atmosphere. During the calcination step, the γ-Fe_3O_4 nanoparticles (dark brown solid) were changed to α-Fe_2O_3 (brown orange solid) as it has been reported by some other research groups.[35] Finally, 10-(3-(trimethoxysilyl)propyl)-2,3,4,6,7,8,9,10-octahydropyrimido[1,2-*a*]azepine (**8**) and MCM-41-coated α-Fe_2O_3 nanoparticles (**11**) were refluxed in toluene in the presence of pyridine and MCM-41-coated nanosized hematite (DBU-F-MCM-41-CNSH) was obtained as a brown orange solid (**12**) (Scheme 3). The freshly synthesized DBU-F-MCM-41-CNSH was characterized by various techniques such as FT-IR, XRD, HR-TEM, FESEM, BET, VSM and elemental analyses (CHN and ICP-OES).

In the FT-IR spectrum of synthesized DBU-F-MCM-41-CNSH (**12**), the peak in the region of 550–630 cm^{-1} is attributed to the stretching vibrations of the Fe–O bonds in α-Fe_2O_3 and the peak at about 1080–1200 cm^{-1} belongs to Si–O stretching vibrations. The weak peak appearing at 1463 cm^{-1} is due to the bending vibration of the C–H bonds. The peak at 1645 cm^{-1} is assigned to the stretching vibration of the C=N bonds. The peaks around 2930 cm^{-1} are related to stretching vibrations of the sp^3 C–H bonds. The broad peak appearing at 3429 cm^{-1} is attributed to the stretching vibrations of O–H bonds on the surface of MCM-41 (ESI,† Fig. S2).

The XRD patterns of the freshly synthesized DBU-F-MCM-41-CNSH (**12**) are presented in the ESI,† Fig. S3. The XRD analysis was performed from <2.0° (2θ) to 10.0° (2θ) (ESI,† Fig. S3a) and 20.0° (2θ) to 80.0° (2θ) (ESI,† Fig. S3b). In the low angle XRD, the main peak related to the [100] reflection of DBU-F-MCM-41-CNSH (**12**) as a main characteristic of mesoporous compounds is observed at 2θ = 2.20°. In addition, the XRD pattern in the region of 20.0° (2θ) to 80.0° (2θ) confirmed that the change in the sample color from dark brown to brown orange after calcination of the catalyst is due to the oxidation of embedded γ-Fe_3O_4 to α-Fe_2O_3 nanoparticles.

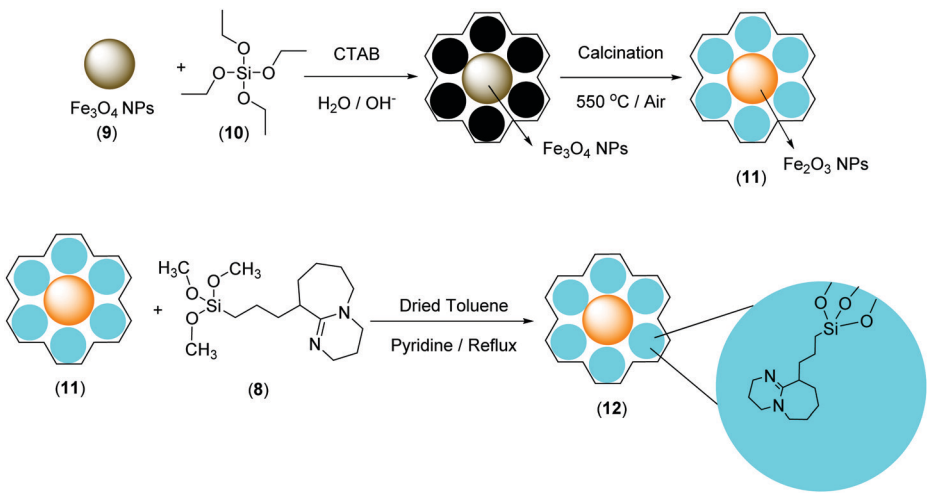

Scheme 3 The synthesis of DBU-F-MCM-41-CNSH (**12**).

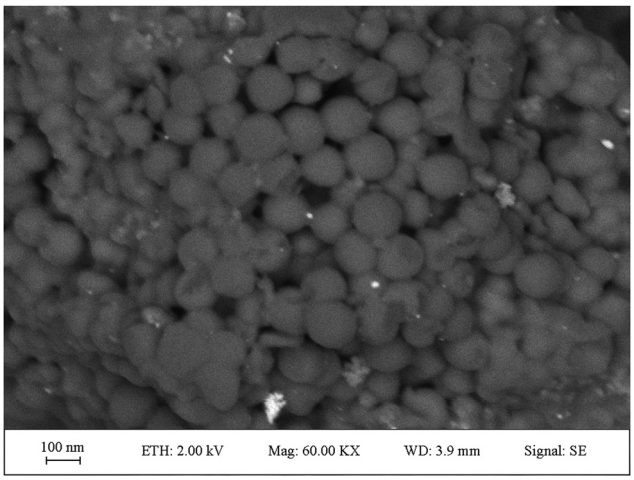

Fig. 1 The FESEM image of synthesized DBU-F-MCM-41-CNSH (**12**).

In order to investigate the morphology and particle size of the synthesized DBU-F-MCM-41-CNSH (**12**), field emission scanning electron microscopy (FESEM) was performed and the result is depicted in Fig. 1. The FESEM image shows approximately uniform and spherical nanoparticles with sizes <100 nm.

The mesostructure of the synthesized DBU-F-MCM-41-CNSH (**12**) was investigated by high resolution transmission electron microscopy (HR-TEM) and the results are depicted in Fig. 2. In the HR-TEM images, the porosity of the sample is observed in the range of mesoporous materials. Moreover, the HR-TEM images show the embedded cores of the α-Fe_2O_3 nanoparticles.

The nitrogen adsorption–desorption isotherms of pure MCM-41 (previously prepared by our research group), MCM-41-coated α-Fe_2O_3 magnetic NPs (**11**) and DBU-F-MCM-41-CNSH (**12**) are exhibited in Fig. 3 and the textural properties are summarized in Table 1.

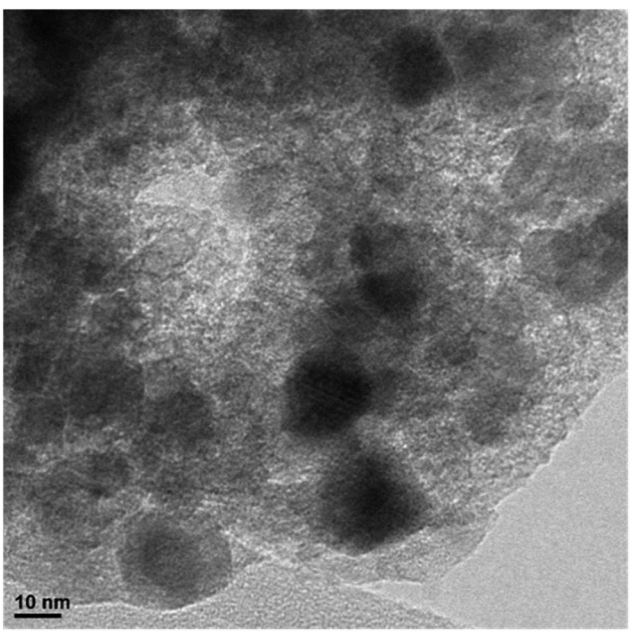

Fig. 2 The HR-TEM images of synthesized DBU-F-MCM-41-CNSH (**12**).

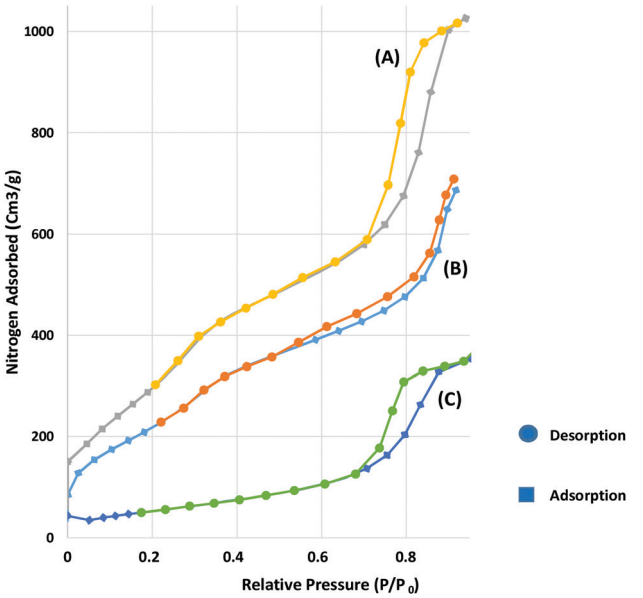

Fig. 3 The nitrogen adsorption–desorption isotherms of MCM-41 (A), MCM-41-coated α-Fe_2O_3 magnetic NPs (B) and DBU-F-MCM-41-CNSH (C).

Table 1 The obtained textural properties of the prepared samples from nitrogen adsorption–desorption isotherms

Sample	BET surface area (m^2 g^{-1})	Average pore diameters (nm)
MCM-41	1177.72	2.47
MCM-41-coated α-Fe_2O_3 magnetic NPs (**11**)	847.67	2.31
DBU-F-MCM-41-CNSH (**12**)	205.33	2.01

The reported results in Table 1 show that the BET surface area and pore diameter of MCM-41 are substantially decreased by the insertion of α-Fe_2O_3 in the MCM-41 framework from 1177 m^2 g^{-1} and 2.47 nm to 847 m^2 g^{-1} and 2.31 nm respectively. Similarly, the BET surface area and pore diameter of the final catalyst (DBU-F-MCM-41-CNSH) are decreased by immobilization of (3-(trimethoxysilyl)propyl)-2,3,4,6,7,8,9,10-octahydropyrimido-[1,2-*a*]azepine (**8**) on the surface of MCM-41-coated α-Fe_2O_3 magnetic nanoparticles (**11**) from 847 m^2 g^{-1} and 2.31 nm to 205 m^2 g^{-1} and 2.01 nm respectively. This result confirms the insertion of magnetic nanoparticles in the framework of MCM-41 and also immobilization of (3-(trimethoxysilyl)propyl)-2,3,4,6,7,8,9,10-octahydropyrimido[1,2-*a*]azepine (**8**) on the surface of the prepared magnetic support (**11**).

Magnetic measurements were carried out using a vibrating sample magnetometer instrument (VSM) at 300 K. The magnetization curves were measured and magnetization *versus* applied magnetic field is shown for the MCM-41-coated α-Fe_2O_3 magnetic NPs (**11**) (A) and DBU-F-MCM-41-CNSH (**12**) (B) in Fig. 4. There was no hysteresis in the magnetization of both examined samples. The saturation magnetization value of the nanoparticles was found to be equal to 4 and 2 emu g^{-1} for the MCM-41-coated α-Fe_2O_3 magnetic NPs (**11**) and DBU-F-MCM-41-CNSH (**12**) respectively, suggesting their superparamagnetic

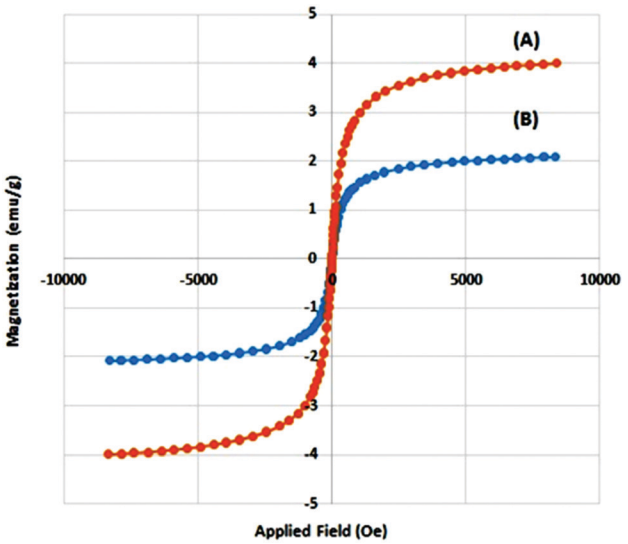

Fig. 4 The magnetization *versus* applied magnetic field curve for MCM-41-coated α-Fe_2O_3 magnetic NPs (**11**) (A) and DBU-F-MCM-41-CNSH (**12**) (B).

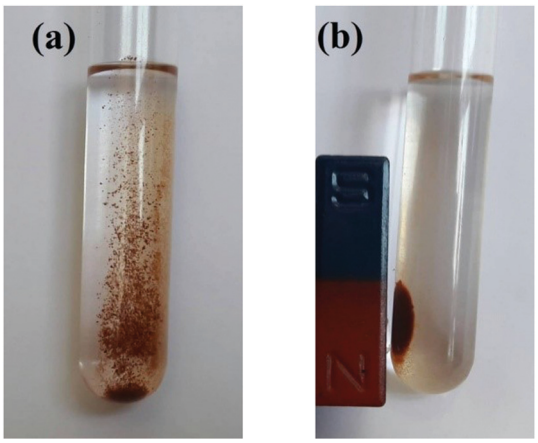

Fig. 5 The magnetic separability of DBU-F-MCM-41-CNSH (**12**): (a) DBU-F-MCM-41-CNSH (**12**) in the reaction mixture and (b) DBU-F-MCM-41-CNSH (**12**) in the presence of an external magnet.

properties. The saturation magnetization value of DBU-F-MCM-41-CNSH (**12**) (2 emu g^{-1}) is lower than that value for the MCM-41-coated α-Fe_2O_3 magnetic NPs (**11**) (4 emu g^{-1}) due to the relatively lower magnetization per unit of mass in the former sample and this also verifies the immobilization of (3-(trimethoxysilyl)propyl)-2,3,4,6,7,8,9,10-octahydropyrimido[1,2-*a*]azepine (**8**) on the surface of the prepared magnetic support (**11**).

Additionally, the magnetic separability of DBU-F-MCM-41-CNSH (**12**) is further studied in reaction media through a separation and re-dispersion process by placing an external magnet near the reaction mixture vessel. The magnetic NPs were attracted towards the magnet within a short period of time, and when the external magnet is removed, they will be re-dispersed in the solution by a slight shake (Fig. 5).

The ICP-OES analysis showed that the Si/Fe molar ratio is equal to 14.45. The results obtained from CHN elemental analysis (%C = 18.01, %H = 2.92, %N = 3.70) reveal that the DBU loading level is equal to 1.25 mmol per gram of the final catalyst.

After the successful preparation and characterization of DBU-F-MCM-41-CNSH (**12**), its catalytic activity was studied in the one-pot four-componet reaction of aryl aldehydes (**1**), malononitrile (**2**), 1,3-thiazolidinedione (**3**) and amines (**4**) for the synthesis of 2-(*N*-carbamoylacetamide)-substituted 2,3-dihydrothiophenes (**5aa–bi**) (Scheme 1). Initially, in order to find the best reaction conditions for the synthesis of 2-(*N*-carbamoylacetamide)-substituted 2,3-dihydrothiophenes (**5**), the one-pot four-component reaction of 4-chlorobenzlaldehyde (**1a**), malononitrile (**2**), 1,3-thiazolidinedione (**3**) and aniline (**4a**) was selected as a model reaction (Scheme 4). The reaction yield and time were recorded under various reaction conditions including different reaction media, amount of the catalyst and temperature. The obtained results are summarized in Table 2.

At the first step, to find an appropriate reaction medium for the synthesis of the title compounds, the model reaction was examined in several solvents such as THF, CH_2Cl_2, $CHCl_3$, EtOAc, CH_3CN, H_2O, MeOH, EtOH, mixtures of EtOH/H_2O (1 : 1, 1 : 2, 2 : 1 and 1 : 3 v/v) and solvent-free conditions (Table 2, entries 1–13 respectively). As it is clear from Table 2, the best results were obtained in the 1 : 2 v/v mixture of EtOH/H_2O as the reaction medium (Table 2, entry 10). Then, the

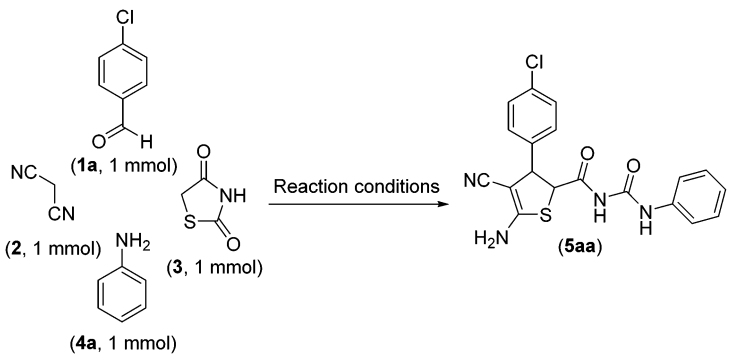

Scheme 4 The one-pot four-component reaction of 4-chlorobenzaldehyde (**1a**, 1 mmol), malononitrile (**2**, 1 mmol), 1,3-thiazolidinedione (**3**, 1 mmol) and aniline (**4a**, 1 mmol) under different conditions.

Table 2 The one-pot four-component reaction of 4-chlorobenzaldehyde (**1a**, 1 mmol), malononitrile (**2**, 1 mmol), 1,3-thiazolidinedione (**3**, 1 mmol) and aniline (**4a**, 1 mmol) under different conditions

Entry	Catalyst (mg)	Solvent (10 mL)	Temp (°C)	Time (min)	Yield[a] (%)
1	DBU-F-MCM-41-CNSH (**20**)	THF	Reflux	240	Trace
2	DBU-F-MCM-41-CNSH (**20**)	CH_2Cl_2	Reflux	240	Trace
3	DBU-F-MCM-41-CNSH (**20**)	CH_3Cl	Reflux	240	Trace
4	DBU-F-MCM-41-CNSH (**20**)	EtOAc	60	240	Trace
5	DBU-F-MCM-41-CNSH (**20**)	CH_3CN	60	240	42
6	DBU-F-MCM-41-CNSH (**20**)	H_2O	60	240	60
7	DBU-F-MCM-41-CNSH (**20**)	MeOH	Reflux	140	78
8	DBU-F-MCM-41-CNSH (**20**)	EtOH	60	110	89
9	DBU-F-MCM-41-CNSH (**20**)	EtOH/H_2O (1 : 1)	60	70	88
10	**DBU-F-MCM-41-CNSH (20)**	**EtOH/H_2O (1 : 2)**	**60**	**40**	**91**
11	DBU-F-MCM-41-CNSH (**20**)	EtOH/H_2O (2 : 1)	60	50	86
12	DBU-F-MCM-41-CNSH (**20**)	EtOH/H_2O (1 : 3)	60	90	81
13	DBU-F-MCM-41-CNSH (**20**)	—	60	240	39
14	DBU-F-MCM-41-CNSH (**5**)	EtOH/H_2O (1 : 2)	60	240	35
15	DBU-F-MCM-41-CNSH (**10**)	EtOH/H_2O (1 : 2)	60	190	82
16	DBU-F-MCM-41-CNSH (**15**)	EtOH/H_2O (1 : 2)	60	110	87
17	DBU-F-MCM-41-CNSH (**25**)	EtOH/H_2O (1 : 2)	60	40	90
18	DBU-F-MCM-41-CNSH (**30**)	EtOH/H_2O (1 : 2)	60	40	92
19	DBU-F-MCM-41-CNSH (**20**)	EtOH/H_2O (1 : 2)	r.t.	240	30
20	DBU-F-MCM-41-CNSH (**20**)	EtOH/H_2O (1 : 2)	40	240	61
21	DBU-F-MCM-41-CNSH (**20**)	EtOH/H_2O (1 : 2)	50	120	89
22	DBU-F-MCM-41-CNSH (**20**)	EtOH/H_2O (1 : 2)	70	40	90
23	DBU-F-MCM-41-CNSH (**20**)	EtOH/H_2O (1 : 2)	80	40	91
24	—	EtOH/H_2O (1 : 2)	60	240	N.R.
25	(α-Fe_2O_3)@MCM-41 (**20**)	EtOH/H_2O (1 : 2)	60	240	Trace

[a] Isolated yields.

optimization process of the reaction conditions was performed by allowing the reaction to proceed using different amounts of DBU-F-MCM-41-CNSH (**12**) as a catalyst (Table 2, entries 10 and 14–18). As the tabulated results show, 20 mg of DBU-F-MCM-41-CNSH (**12**) catalyzed the reaction efficiently and produced a high yield of the product in the shortest reaction time (Table 2, entry 10). An increase of the amount of DBU-F-MCM-41-CNSH (**12**) to more than 20 mg showed no substantial improvement in the yield (Table 2, entries 17 and 18), whereas the yield decreased by reducing the amount of DBU-F-MCM-41-CNSH (**12**) to less than 20 mg (Table 2, entries 14–16). Moreover, it was observed that the reaction did not proceed at all in the absence of DBU-F-MCM-41-CNSH (**12**) even after 240 min (Table 2, entry 24), which shows the essential role of DBU-F-MCM-41-CNSH (**12**) in the improvement of the reaction time and the product yield. Subsequently, the reaction temperature was checked (Table 2, entries 10 and 19–23). From the summarized data in Table 2, the best results were obtained when the reaction temperature was 60 °C (Table 2, entry 10). While increasing the reaction temperature to more than 60 °C did not improve the result in terms of the yields and the reaction times substantially (Table 2, entries 22 and 23), decreasing the reaction temperature to less than 60 °C led to a decrease in the yield and an increase in the reaction time (Table 2, entries 19–21). In the final stage, to show the impact and efficiency of the support on the catalytic activity of DBU-F-MCM-41-CNSH (**12**), the model reaction was carried out in the presence of 20 mg of MCM-41-coated α-Fe_2O_3 magnetic NPs (**11**) under the same conditions and a trace yield of the product compared to the optimized reaction conditions was obtained after 240 min (Table 2, entry 25). Therefore, after a comprehensive exploration, the best yield and time profile for the model reaction were obtained with the use of 20 mg of DBU-F-MCM-41-CNSH (**12**) in a 1 : 2 v/v mixture of EtOH/H_2O at 60 °C, which led to the production of the corresponding 2-(*N*-carbamoylacetamide)-substituted 2,3-dihydrothiophene (**5aa**) in 91% yield within 40 min (Table 2, entry 10).

Encouraged by the remarkable optimization results, we decided to utilize various aryl aldehydes (**1**) and amines (**4**) with malononitrile (**2**) and 1,3-thiazolidinedione (**3**) to investigate the scope, efficiency and generality of the synthesized catalyst (DBU-F-MCM-41-CNSH (**12**)) for the synthesis of 2-(*N*-carbamoylacetamide)-substituted 2,3-dihydrothiophenes (**5**) (Scheme 1) and the obtained results are summarized in Table 3.

As Table 3 illustrates, all reactions proceeded efficiently and the desired products were produced in good to excellent yields (83–94%) and in relatively short reaction times (25–45 min) without formation of any organic side products. Although, aryl aldehydes (**1**) substituted with electron withdrawing groups (Table 3, entries 7, 10, 23, 29 and 35) reacted at faster rates

Table 3 The one-pot four-component reaction of aryl aldehydes (**1**, 1 mmol), malononitrile (**2**, 1 mmol), 1,3-thiazolidinedione (**3**, 1 mmol) and amines (**4**, 1 mmol) under the optimized conditions

Entry	Ar	R^1	R^2	Product	Time (min)	Yield[a] (%)
1	4-Cl-Ph	H	Ph	**5aa**	40	91
2	4-Br-Ph	H	Ph	**5ab**	45	89
3	4-Me-Ph	H	Ph	**5ac**	45	89
4	3-Me-Ph	H	Ph	**5ad**	40	90
5	4-*t*Bu-Ph	H	Ph	**5ae**	45	90
6	4-Ome-Ph	H	Ph	**5af**	45	89
7	3-NO_2-Ph	H	Ph	**5ag**	35	92
8	4-Me-Ph	H	4-Cl-Ph	**5ah**	45	90
9	3-Me-Ph	H	4-Cl-Ph	**5ai**	40	92
10	4-F-Ph	H	4-Cl-Ph	**5aj**	35	93
11	Ph	H	3-Cl-Ph	**5ak**	40	91
12	4-Br-Ph	H	3-Cl-Ph	**5al**	45	88
13	4-iPr-Ph	H	3-Cl-Ph	**5am**	45	87
14	4-Me-Ph	H	3-Br-Ph	**5an**	45	87
15	Ph	H	4-Me-Ph	**5ao**	35	92
16	4-Cl-Ph	H	4-Me-Ph	**5ap**	35	91
17	4-Ome-Ph	H	4-Me-Ph	**5aq**	40	90
18	4-Cl-Ph	H	4-OMe-Ph	**5ar**	35	92
19	3-Me-Ph	H	4-OMe-Ph	**5as**	35	90
20	3-NO_2-Ph	H	4-OMe-Ph	**5at**	30	94
21	Ph	H	3-OMe-Ph	**5au**	35	91
22	4-*t*Bu-Ph	H	3-OMe-Ph	**5av**	40	87
23	3-NO_2-Ph	H	3-OMe-Ph	**5aw**	30	93
24	Ph	H	4-OEt-Ph	**5ax**	35	93
25	Ph	H	$-CH_2CH_2CH_2CH_3$	**5ay**	35	84
26	4-Cl-Ph	$-CH_2CH_2CH_2CH_2CH_2-$		**5az**	30	87
27	2-Cl-Ph	$-CH_2CH_2CH_2CH_2CH_2-$		**5ba**	30	86
28	3-Me-Ph	$-CH_2CH_2CH_2CH_2CH_2-$		**5bb**	35	87
29	3-NO_2-Ph	$-CH_2CH_2CH_2CH_2CH_2-$		**5bc**	25	88
30	4-Cl-Ph	$-CH_2CH_2OCH_2CH_2-$		**5bd**	30	89
31	4-Me-Ph	$-CH_2CH_2OCH_2CH_2-$		**5be**	35	86
32	4-Ome-Ph	$-CH_2CH_2OCH_2CH_2-$		**5bf**	35	85
33	1-Thienyl	$-CH_2CH_2OCH_2CH_2-$		**5bg**	35	89
34	4-Cl-Ph	$-CH_2CH_2N(Ph)CH_2CH_2-$		**5bh**	45	83
35	3-NO_2-Ph	$-CH_2CH_2N(Ph)CH_2CH_2-$		**5bi**	40	85

[a] Isolated yields.

compared to aryl aldehydes (**1**) having electron releasing groups (Table 3, entries 6, 17 and 32). Furthermore, this protocol is not sensitive to steric hindrance in terms of yield and reaction time (Table 3, entry 27). Besides, thiophene-2-carboxaldehyde, which is an acid-sensitive heteroaromatic aldehyde, also was employed successfully in this method (Table 3, entry 33). To broaden the scope of the reaction, diverse aromatic and aliphatic amines were also employed and afforded the desired products. Nonetheless, when aliphatic amines were used, the yields were increased a little and the reaction times were slightly shorter in comparison with aromatic amines.

To explain the mechanism of this one-pot four-component reaction of aryl aldehydes (**1**), malononitrile (**2**), 1,3-thiazolidinedione (**3**) and amines (**4**) and the formation of 2-(*N*-carbamoylacetamide)-substituted 2,3-dihydrothiophenes (**5aa–bi**) in the presence of DBU-F-MCM-41-CNSH (**12**), we propose a plausible reaction mechanism, which is illustrated in Scheme 5.

The first step is the DBU-F-MCM-41-CNSH (**12**) catalyzed formation of arylidenemalononitrile (**13**) derived from the Knoevenagel condensation of the aromatic aldehyde (**1**) with malononitrile (**2**) after removing one molecule of water. In the next step, 1,3-thiazolidinedione (**3**) in the presence of DBU-F-MCM-41-CNSH (**12**) converts to its corresponding enolate (**3a**) and adds to the arylidenemalononitrile (**13**) by Michael reaction to produce a 1,3-thiazolidinedione-containing intermediate (**14**). Then, the amine (**4**) attacks the carbonyl group of the 1,3-thiazolidinedione moiety of the 1,3-thiazolidinedione-containing intermediate (**14**) to open its ring and cause the formation of a thiol-containing intermediate (**15**), which in turn intramolecularly attacks one of the two cyano groups to form a sulfur-containing five-membered ring intermediate (**16**). After this, the desired product was produced by an imine–enamine tautomeric proton shift.

This is noteworthy that there is sometimes more than one possible reaction pathway for MCRs.[36] In order to check the authenticity of the suggested mechanistic pathway for the one-pot four-component reaction of aryl aldehydes (**1**), malononitrile (**2**), 1,3-thiazolidinedione (**3**) and amines (**4**) in the presence of DBU-F-MCM-41-CNSH in EtOH/H_2O 1 : 2 v/v at 60 °C (Scheme 5), a number of separate experiments were designed and performed. Firstly, 4-chlorobenzaldehyde (**1a**, 1 mmol) was reacted with malononitrile (**2**, 1 mmol) in the presence of DBU-F-MCM-41-CNSH (**12**, 20 mg) in EtOH/H_2O 1 : 2 v/v (10 mL) at 60 °C and the 2-(4-chlorobenzylidene)malononitrile (**13b**) was obtained in 98% yield after 5 min (Scheme 6a).[38] In the next step, the possibility of the Michael addition of 1,3-thiazolidinedione (**3**) to the arylidenemalononitrile (**13**) in the presence of DBU-F-MCM-41-CNSH (**12**) was checked. For this, the freshly synthesized

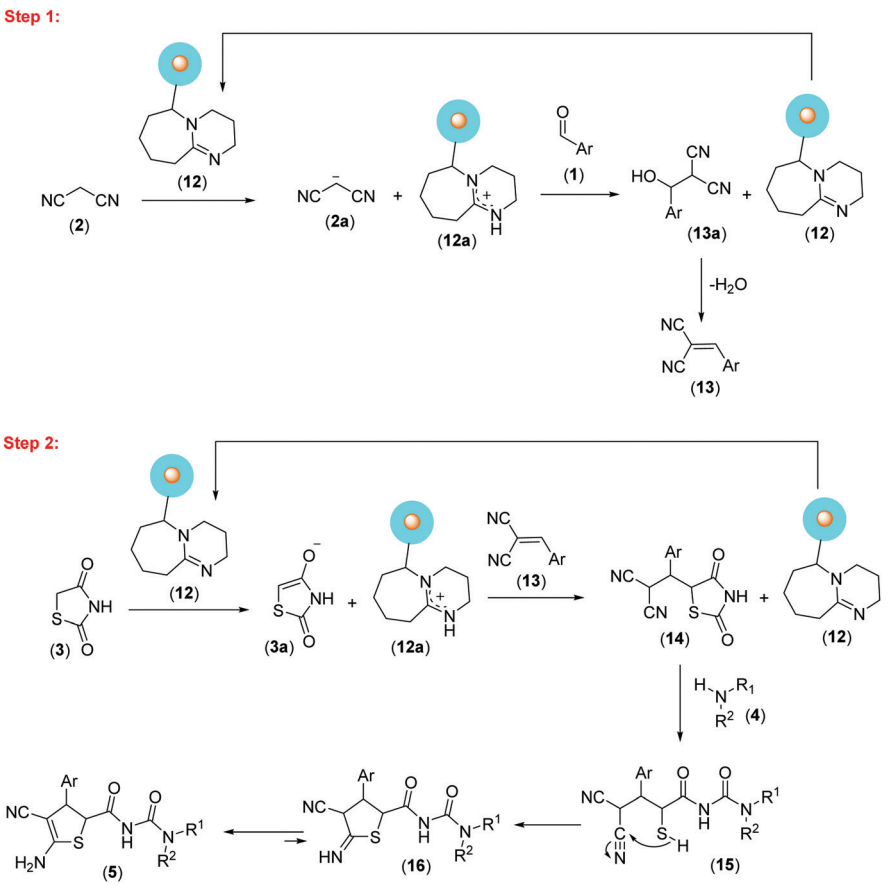

Scheme 5 A plausible mechanism for the one-pot four-component reaction of aryl aldehydes (**1**), malononitrile (**2**), 1,3-thiazolidinedione (**3**) and amines (**4**) in the presence of DBU-F-MCM-41-CNSH in EtOH/H_2O 1 : 2 v/v at 60 °C.

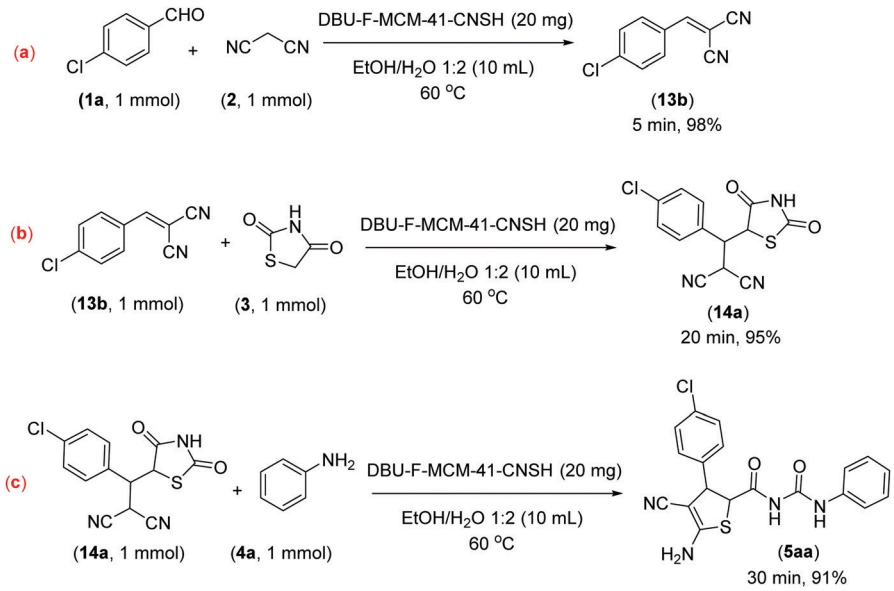

Scheme 6 The study of the authenticity of the proposed reaction pathway for the one-pot four-component reaction of aryl aldehydes (**1**), malononitrile (**2**), 1,3-thiazolidinedione (**3**) and amines (**4**) in the presence of DBU-F-MCM-41-CNSH in EtOH/H_2O 1 : 2 v/v at 60 °C.

2-(4-chlorobenzylidene)malononitrile (1 mmol) was treated with 1,3-thiazolidinedione (**3**, 1 mmol) in the presence of DBU-F-MCM-41-CNSH (**12**, 20 mg) in EtOH/H_2O 1 : 2 v/v (10 mL) at 60 °C and, as expected, 2-((4-chlorophenyl)(2,4-dioxothiazolidin-5-yl)methyl)malononitrile (**14a**) was obtained in 95% yield after 20 min (Scheme 6b). Finally, the synthesized 2-((4-chlorophenyl)-(2,4-dioxothiazolidin-5-yl)methyl)malononitrile (**14a**, 1 mmol) was treated with aniline (**4a**, 1 mmol) under the optimized reaction conditions and the desired product (**5aa**) was obtained in 91% isolated yield after 30 min.

Apparently, there are four feasible stereoisomers of the synthesized compounds (*trans* and *cis*). As an X-ray crystallography facility was not accessible to us, we compared the ^{1}H-NMR data of the synthesized compounds with reported compounds whose structures have been characterized with X-ray crystallography. It can be concluded that the *trans* diastereomer is the real and also the only structure that formed during the synthesis of the title compounds in the presence of DBU-F-MCM-41-CNSH (**12**) under optimized conditions.[37] To explain the reason for the diastereoselectivity, it can be stated that at the cyclization step which has already been discussed, the sterically large 3-aryl and 2-ureidoformamide groups prefer stereochemically opposite positions to reduce the steric hindrance in the thiol group and in the transition state of that step (Scheme 7). Thus, only the *trans* isomeric 2-(*N*-carbamoylacetamide)-substituted 2,3-dihydrothiophene was produced after cyclization.

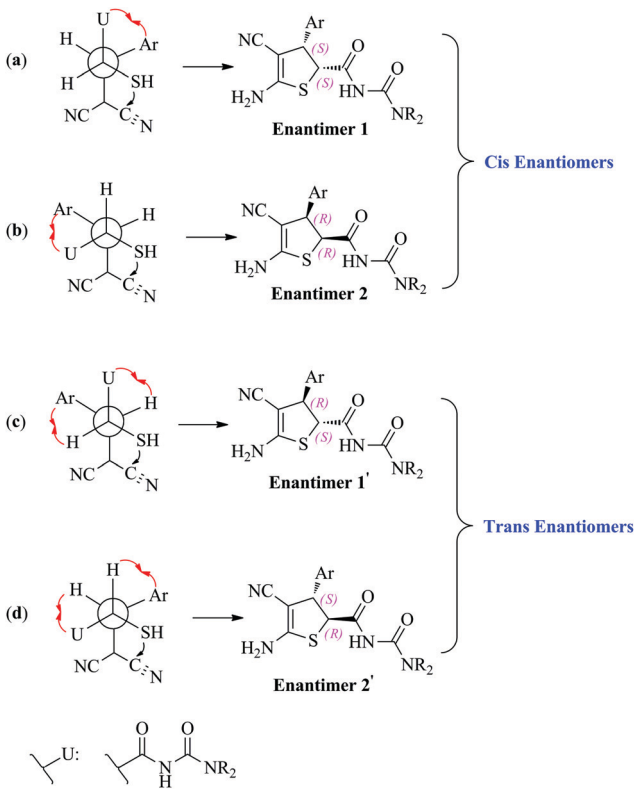

Scheme 7 The feasible stereoisomers of 2-(*N*-carbamoylacetamide)-substituted 2,3-dihydrothiophene.

The possibility of recycling the catalyst was examined using the model reaction under the optimized conditions. After the completion of the reaction, as indicated by TLC, the reaction mixture was cooled to room temperature and filtered. The separated solids were dissolved in hot ethanol (20 mL) and the remaining insoluble catalysts were separated using an external magnet. The small amount of catalyst that passed the filter also was separated using an external magnet and added to the separated catalyst from the hot ethanol, washed well with hot ethanol (5 mL, 2 times), dried at 120 °C and kept for another use. The recovered catalyst was reused eight times in the model reaction under the optimized conditions without any loss of catalytic activity (Fig. 6).

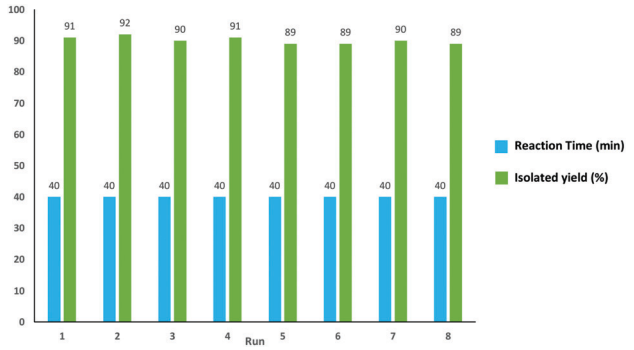

Fig. 6 The one-pot four-component reaction of 4-chlorobenzaldehyde (**1a**, 1 mmol), malononitrile (**2**, 1 mmol), 1,3-thiazolidinedione (**3**, 1 mmol) and aniline (**4a**, 1 mmol) in the presence of recovered DBU-F-MCM-41-CNSH (**12**) under the optimized conditions.

In order to investigate the chemical and physical stability of the catalyst, its chemical and physical structure was studied using FT-IR, XRD, HR-TEM, FESEM, BET and elemental analyses (CHN and ICP-OES) after the 8th reuse.

As can be seen in the ESI,† Fig. S4, there are no significant differences between the FT-IR spectrum of the recovered catalyst after the 8th reuse and the FT-IR spectrum of the freshly synthesized catalyst shown in the ESI,† Fig. S2.

XRD analysis was performed from $<2.0^{\circ}$ (2θ) to 10.0° (2θ) for the recovered catalyst after the 8th reuse (ESI,† Fig. S5). Obviously, there are not any discernible differences between the XRD pattern of the recovered catalyst after the 8th reuse and that of the freshly synthesized catalyst shown in the ESI,† Fig. S3a.

The FESEM image of the recovered catalyst after the 8th reuse shows uniform and spherical encapsulated nanoparticles with sizes <100 nm (Fig. 7) and this demonstrates that the catalyst retains its unique morphology even after the 8th reuse.

In the HR-TEM image, the porosity of the recovered catalyst after the 8th reuse is still observed in the range of mesoporous materials (Fig. 8) and similar to the HR-TEM image of the freshly synthesized catalyst shown in Fig. 5 embedded cores of α-Fe_2O_3 nanoparticles can be still seen.

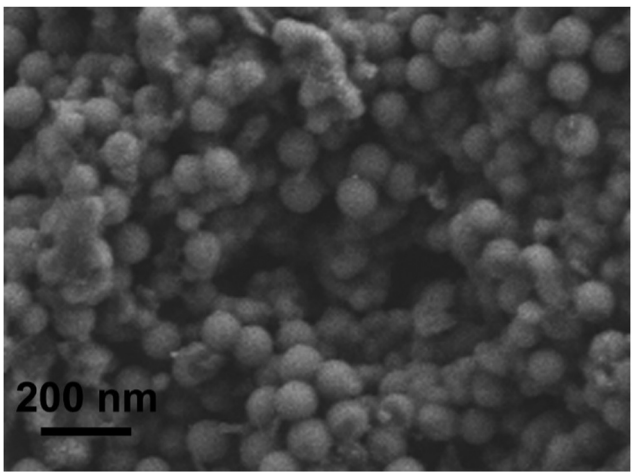

Fig. 7 The FESEM image of the recovered DBU-F-MCM-41-CNSH after the 8th reuse.

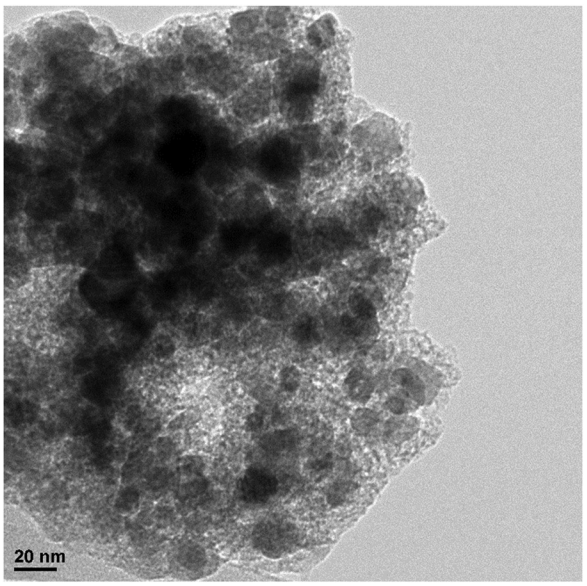

Fig. 8 The HR-TEM images of the recovered DBU-F-MCM-41-CNSH after the 8th reuse.

The textural properties of the recovered catalyst after the 8th reuse were studied by the BET method. The nitrogen adsorption–desorption isotherms of the recovered catalyst after the 8th reuse are presented in Fig. 9 and the textural properties summarized in Table 4. The obtained textural properties of the recovered catalyst after the 8th reuse from nitrogen adsorption–desorption isotherms approximate the textural properties of the freshly synthesized catalyst.

The ICP-OES analysis of the recovered catalyst after the 8th reuse showed that the Si/Fe molar ratio is equal to 14.38, which is so close to the same ratio as the freshly synthesized

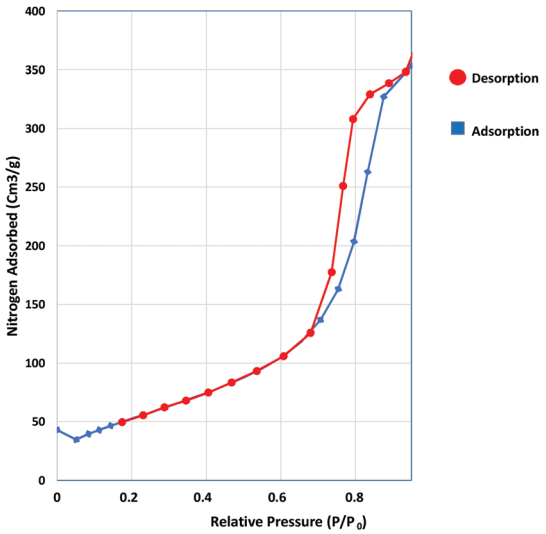

Fig. 9 The nitrogen adsorption–desorption isotherms of the recovered DBU-F-MCM-41-CNSH after the 8th reuse.

Table 4 The obtained textural properties of the recovered DBU-F-MCM-41-CNSH after the 8th reuse from nitrogen adsorption–desorption isotherms

Sample	BET surface area (m^2 g^{-1})	Average pore diameters (nm)
DBU-F-MCM-41-CNSH after the 8th reuse	201.69	2.05

catalyst (Si/Fe = 14.45). The results obtained from CHN elemental analysis (%C = 18.30, %H = 3.06, %N = 3.15) are also close to the CHN elemental analysis of the freshly synthesized catalyst (%C = 18.01, %H = 2.92, %N = 3.70). So it is shown by the obtained results that the physical and chemical structures of DBU-F-MCM-41-CNSH are stable under the applied conditions even after eight times of reuse.

Conclusions

First of all, DBU was converted from a volatile, highly toxic and non-recoverable liquid to a new, highly efficient, magnetically separable and reusable nano-sized mesoporous solid base catalyst. The catalytic activity of the synthesized DBU-functionalized magnetically separable mesoporous material was very well proved with the conduction of the one-pot four-component synthesis of 2-(*N*-carbamoylacetamide)-substituted 2,3-dihydrothiophenes in short times (25–45 min) and with good to excellent yields (83–94%). The other promising points of the presented methodology are operational simplicity, mild reaction conditions, a clean reaction profile, a versatile range of available substrates and as a consequence high diversity of the products, enhanced rates, high isolated yields of the pure products, diasteroselectivity, no formation of by-products, chemical and physical stability of the catalyst, easy recovery and reusability of the catalyst and finally agreement with some of the Green Chemistry protocols.

Conflicts of interest

There are no conflicts to declare.

Acknowledgements

Thanks are due to the Shiraz University Research Councils and Iran's National Science Foundation (INSF) for supporting this work.

Notes and references

1 *Multicomponent Reactions in Organic Synthesis*, ed. J. Zhu, Q. Wang and M.-X. Wang, Wiley-VCH, Weinheim, Germany, 2015.
2 T. J. Müller, *Science of Synthesis, Multicomponent Reactions*, Thieme, Stutgart, Germany, 2014, vol. 1 and 2.
3 F. de Moliner, N. Kielland, R. Lavilla and M. Vendrell, *Angew. Chem., Int. Ed.*, 2017, **56**, 3758.
4 D. G. Hall, T. Rybak and T. Verdelet, *Acc. Chem. Res.*, 2016, **49**, 2489.
5 (*a*) B. B. Toure and D. G. Hall, *Chem. Rev.*, 2009, **109**, 4439; (*b*) M. M. Khan, S. Khan and S. Iqbal, *RSC Adv.*, 2016, **6**, 42045; (*c*) M. M. Khan, R. Yousuf and S. Khan, *RSC Adv.*, 2015, **5**, 57883; (*d*) J.-P. Wan and Y. Liu, *RSC Adv.*, 2012, **2**, 9763; (*e*) L. El Kaim and L. Grimaud, *Eur. J. Org. Chem.*, 2014, 7749; (*f*) V. Estevez, M. Villacampa and J. C. Menendez, *Chem. Soc. Rev.*, 2014, **43**, 4633; (*g*) S. Brauch, S. S. van Berkel and B. Westermann, *Chem. Soc. Rev.*, 2013, **42**, 4948; (*h*) L. Banfi, A. Basso, L. Moni and R. Riva, *Eur. J. Org. Chem.*, 2014, 2005; (*i*) M. Jose Climent, A. Corma and S. Iborra, *RSC Adv.*, 2012, **2**, 16; (*j*) B. H. Rotstein, S. Zaretsky, V. Rai and A. K. Yudin, *Chem. Rev.*, 2014, **114**, 8323; (*k*) M. Mahfoudh, R. Abderrahim, E. Leclerc and J. M. Campagne, *Eur. J. Org. Chem.*, 2017, 2856; (*l*) H. G. O. Alvim, J. R. Correa, J. A. F. Assumpcą, W. A. da Silva, M. O. Rodrigues, J. L. de Macedo, M. Fioramonte, F. C. Gozzo, C. C. Gatto and B. A. D. Neto, *J. Org. Chem.*, 2018, **83**, 4044; (*m*) E. M. de Marigorta, J. M. de los Santos, M. O. de Retana and J. Vicario, *Synthesis*, 2018, 4539; (*n*) M. Konstantinidou, K. Kurpiewska, J. Kalinowska-Tłuscik and A. Dömling, *Eur. J. Org. Chem.*, 2018, 6714; (*o*) S. Yu, R. Hua, X. Fu, G. Liu, D. Zhang, Sh. Jia, H. Qiu and W. Hu, *Org. Lett.*, 2019, **21**, 5737.
6 M. Wen, P.-P. Sun, X. Luo and W.-P. Deng, *Tetrahedron*, 2018, **74**, 4168.
7 P. Gopinath and S. Chandrasekaran, *J. Org. Chem.*, 2010, **76**, 700.
8 A. Kumar, G. Gupta and S. Srivastava, *Green Chem.*, 2011, **13**, 2459.
9 H. Maruoka, M. Yamazaki and Y. Tomioka, *J. Heterocycl. Chem.*, 2004, **41**, 641.
10 V. Dotsenko, S. Krivokolysko and V. Litvinov, *Russ. Chem. Bull.*, 2009, **58**, 1524.
11 J. Sun, L.-L. Zhang, E.-Y. Xia and C.-G. Yan, *J. Org. Chem.*, 2009, **74**, 3398.
12 D. Q. Shi, Y. Zou, Y. Hu and H. Wu, *J. Heterocycl. Chem.*, 2011, **48**, 896.
13 G.-p. Lu, L.-Y. Zeng and C. Cai, *Green Chem.*, 2011, **13**, 998–1003.
14 J. Sun, E. Xia, L. Zhang and C. Yan, *Sci. China: Chem.*, 2010, **53**, 863.
15 J. Sun, E. Y. Xia, L. L. Zhang and C. G. Yan, *Eur. J. Org. Chem.*, 2009, 5247.
16 J. Sun, E.-Y. Xia, R. Yao and C.-G. Yan, *Mol. Diversity*, 2011, **15**, 115.
17 R. Yao, E. Xia, J. Sun and C. Yan, *Chin. J. Chem.*, 2011, **29**, 2461.
18 A. K. Bagdi, S. Santra, K. Monir and A. Hajra, *Chem. Commun.*, 2015, **51**, 1555.
19 A. Domling, W. Wang and K. Wang, *Chem. Rev.*, 2012, **112**, 3083.
20 V. Polshettiwar and R. S. Varma, *Green Chem.*, 2010, **12**, 743.
21 J. L. Chiara, L. Encinas and B. Díaz, *Tetrahedron Lett.*, 2005, **46**, 2445.

22 E. Quaranta, A. Angelini, M. Carafa, A. Dibenedetto and V. Mele, *ACS Catal.*, 2013, **4**, 195.
23 R. Baharfar and N. Shariati, *Turk. J. Chem.*, 2015, **39**, 235–243.
24 L. Zhang, Y. Li and H. Zhou, *Energy*, 2018, **149**, 414.
25 D. Wang and D. Astruc, *Chem. Rev.*, 2014, **114**, 6949.
26 M. Wen, P.-P. Sun, X. Luo and W.-P. Deng, *Tetrahedron*, 2018, **74**, 4168.
27 V. Polshettiwar and R. S. Varma, *Green Chem.*, 2010, **12**, 743.
28 J. L. Chiara, L. Encinas and B. Díaz, *Tetrahedron Lett.*, 2005, **46**, 2445.
29 E. Quaranta, A. Angelini, M. Carafa, A. Dibenedetto and V. Mele, *ACS Catal.*, 2013, **4**, 195.
30 R. Baharfar and N. Shariati, *Turk. J. Chem.*, 2015, **39**, 235.
31 L. Zhang, Y. Li and H. Zhou, *Energy*, 2018, **149**, 414.
32 D. Wang and D. Astruc, *Chem. Rev.*, 2014, **114**, 6949.
33 (*a*) A. Moaddeli, M. Rousta, M. Shekouhy, D. Khalili, M. Samadi and A. Khalafi-Nezhad, *Asian J. Org. Chem.*, 2019, **8**, 356; (*b*) M. Shekouhy, R. Kordnezhadian and A. Khalafi-Nezhad, *J. Iran. Chem. Soc.*, 2018, **15**, 2357; (*c*) H. R. Safaei, M. Shekouhy and S. Ghorbanzadeh, *ChemistrySelect*, 2018, **3**, 4750; (*d*) M. Shekouhy, A. Moaddeli and A. Khalafi-Nezhad, *J. Porous Mater.*, 2018, **25**, 75; (*e*) M. Shekouhy, A. Moaddeli and A. Khalafi-Nezhad, *J. Ind. Eng. Chem.*, 2017, **50**, 41; (*f*) M. Shekouhy, A. Moaddeli and A. Khalafi-Nezhad, *Res. Chem. Intermed.*, 2016, **42**, 3805; (*g*) H. R. Safaei, M. Safaei and M. Shekouhy, *RSC Adv.*, 2015, **5**, 6797; (*h*) H. R. Safaei, M. Shekouhy, V. Shafiee and M. Davoodi, *J. Mol. Liq.*, 2013, **180**, 139.
34 M. Shekouhy and A. Khalafi-Nezhad, *Green Chem.*, 2015, **17**, 4815.
35 S. Rostamizadeh, M. Azad, N. Shadjou and M. Hasanzadeh, *Catal. Commun.*, 2012, **25**, 83.
36 L. M. Ramos, M. O. Rodrigues and B. A. D. Neto, *Org. Biomol. Chem.*, 2019, **17**, 7260.
37 J. Sun, E. Y. Xia, L. L. Zhang and C. G. Yan, *Eur. J. Org. Chem.*, 2009, 5247.
38 R. Khoshnavazi, L. Bahrami and F. Havasi, *RSC Adv.*, 2016, **6**, 100962.

